Membrane lipid segregation in endocytosis

Sarah A. Nowak[1] and Tom Chou[1,2]
[1]*Department of Biomathematics, David Geffen School of Medicine, UCLA, Los Angeles, California 90095-1766, USA*
[2]*Department of Mathematics, UCLA, Los Angeles, California 90095-1555, USA*
(Received 27 January 2008; published 18 August 2008)

We explore the equilibrium mechanics of a binary lipid membrane that wraps around a spherical or cylindrical particle. One of the lipid membrane components induces a positive spontaneous curvature, while the other induces a negative local curvature. Using a Hamiltonian approach, we derive the equations governing the membrane shape and lipid concentrations near the wrapped object. Asymptotic expressions and numerical solutions for membrane shapes are presented. We determine the regimes of bending rigidity, surface tension, intrinsic lipid curvature, and effective receptor binding energies that lead to efficient wrapping and endocytosis. Our model is directly applicable to the study of invagination of clathrin-coated pits and receptor-induced wrapping of colloids such as spherical virus particles.

DOI: 10.1103/PhysRevE.78.021908 PACS number(s): 87.10.−e, 87.16.dt, 87.16.dm, 45.20.Jj

I. INTRODUCTION

The cell membrane is more than a static barrier that passively separates the cytoplasm from the extracellular environment. Rather, cellular membranes mediate signaling and undergo dynamic remodeling to enable intra- and extracellular transport. For example, cells can secrete signaling molecules via exocytosis, viruses can enter host cells through endocytosis [1] (see Fig. 1), and organelles can package proteins for intracellular transport by budding. Enveloped viruses also exit cells by an exocytosis mechanism similar to budding. To understand the physics and dynamics of these processes, which all involve membrane deformation, we must understand the physical properties of the cell membrane. Many modern experimental techniques directly probe the physical properties of the cell membrane. For example, membrane surface tension has been measured using micropipettes [2,3], laser tweezer traps [4], and atomic force microscopy (AFM) protocols [1,5]. Membrane bending rigidity can also be inferred from micropipette experiments [6]. Other investigations have sought to recapitulate membrane remodeling in model *in vitro* systems; the degree of wetting of a latex bead held by an optical trap has been studied as a model system for endocytosis [7].

Membrane heterogeneity is thought to be important not only for biological signaling at the cell surface, but also for the mechanics of cell surface deformation, cell motility, and intracellular transport [8]. Proteins and lipids that alter membrane curvature can mediate membrane deformation. For example, proteins that impart spontaneous curvature can be embedded in the lipid membranes [9], they may bind to the membrane as monomer, which the BAR domain does, or they may polymerize into a curvature-inducing protein coat, which the COPI and COPII complexes do [10]. Other membrane components such as cholesterol [11] and membrane lipids may have an intrinsic curvature. This topic is discussed in depth in [9]. Multicomponent membranes have been observed to phase separate [12], and budding induced by line tension between lipid phase domains has been observed experimentally [13].

Specifically, we explore the effects of membrane heterogeneity, realized by lipids with different intrinsic curvatures, on the mechanics of a membrane binding to either a long cylindrical particle or a spherical particle. The wrapped particle may be a spherical virus, an approximately cylindrical peptide chain, or a protein scaffold. Dynamin and BAR-domain-containing proteins form cylindrical scaffolds while COPI, COPII, and clathrin-adapter protein complexes form spherical intermediate structures [9].

Early theoretical studies of membrane adhesion examined the adsorption of a membrane tubule onto a cylindrical groove [14]. The phase diagram of long tubular membranes

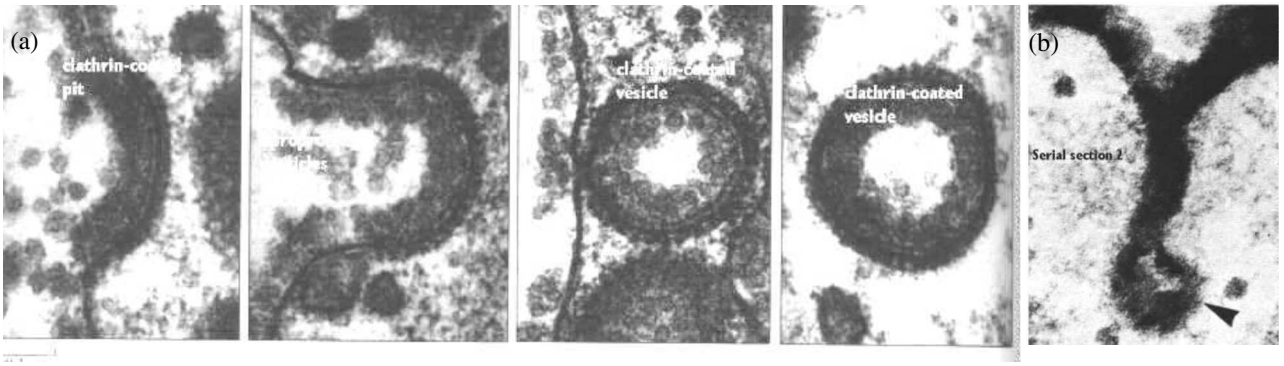

FIG. 1. Endocytosis can involve intermediates of qualitatively different shapes. (a) A clathrin-coated pit with tight wrapping and spherical enclosure. (b) Endocytosis can also involve intermediates with long-tube-like processes. Both figures were taken from [56].

adhering to a flat surface has been described [15] and the force required to remove a long cylindrical bead adhering to a flat membrane has been calculated in the small deformation limit [16]. Adhesion of a spherical particle to a flat membrane has been studied in depth [17,18] as has the adhesion of a vesicle to a curved substrate [19]. In all of these studies, single-component membranes were considered. Multicomponent membranes that are unattached to substrate can assume a variety of shapes; this phenomenon has been explored in two dimensions [20] and in three dimensions for axisymmetric vesicles [21,22]. Phase separation and domain formation in multicomponent membranes has been studied extensively [23–26]. A number of consequences of membrane phase separation have been explored. For example, domain boundaries in membrane tethers have been shown experimentally and theoretically to create weak spots, where the tether can break under tension [27]. Also, budding induced by line tension between lipid phase domains has been described theoretically in both static [28–31] and dynamic [32] cases. Additionally, much work has been done to understand the forces that arise between embedded and bound membrane proteins [33–37] as well as the membrane deformations that may result from these proteins [38–40]. A few studies have considered multicomponent membranes that adhere to substrates. Under some conditions, a membrane that would not ordinarily phase separate will exhibit phase separation upon substrate binding due to the reduction of entropy in the bound region [26]. Entropic effects can also be important in receptor-mediated endocytosis when adhesion of a membrane to a particle is mediated by receptors that diffuse along the membrane and bind to the particle. Studies of this process have shown that the entropic cost of receptor immobilization results in a optimum particle size for efficient endocytosis [41]. Finally, molecular dynamics simulations have demonstrated lipid sorting in a membrane composed of a binary mixture of two lipids where one lipid prefers positive curvature and the other prefers negative curvature upon adhesion to a curved surface [42]. In this paper, we explore this phenomenon both numerically and analytically and consider how the lipid sorting in turn affects membrane adhesion. While there has been much theoretical work on the adhesion of single-component membranes and on multicomponent membranes, little work has been done on adhesion of multicomponent membranes.

To find the equilibrium shape of the cell membrane, we minimize its free energy. We include a Helfrich bending free energy, a surface tension energy, and a free energy arising from local inhomogeneities in lipid composition and use the Hamiltonian approach of [18,21] to derive equations governing membrane shape. In Sec. II and Appendix A, we derive the Euler-Lagrange equations consistent with minimization of the total free energy of a membrane wrapping around cylindrical and spherical particles. Upon solving these equations, the point at which the membrane detaches from the particle and the associated membrane shapes can be found. In Sec. III A, we discuss the limit in which the lipid concentration and the membrane curvature become decoupled, reviewing the results of Deserno [18]. In Sec. III B, we discuss the limit in which concentration curvature coupling is very strong, and present numerical and analytic results. In Sec. IV, we discuss the qualitative effect of phase separation and inhomogeneous Gaussian bending rigidity on membrane shape. Finally, we will summarize and discuss the implications of our findings in Sec. V.

II. CONCENTRATION-COUPLED MEMBRANE MODEL

In this section, we develop the free energy of a two-component membrane as it wraps a rigid particle. The free energy includes contributions from membrane bending (described by the Helfrich free energy [43]), local variations in lipid composition, surface tension, and coupling between lipid composition and local membrane curvature. Biological membranes are primarily composed of lipids that have a polar head and a hydrophobic tail. Lipid membranes have two leaflets and lipids are oriented such that their hydrophobic tails point into the membrane, shielded from the polar environment by the polar head groups, which are on the outside of the membrane. We consider a membrane with two curvature-inducing components: lipid A has a wide tail compared to its head and induces positive curvature in the top membrane leaflet, and lipid B has a has a wider head than tail and induces negative intrinsic curvature in the top membrane leaflet. Lipids A and B may be the only components of the membrane, or they may be mixed with other lipid species that lack intrinsic curvature. We define the order parameter $\phi=\phi_A-\phi_B$ where ϕ_A and ϕ_B are the area fractions of lipid A and lipid B. We also assume that the lipid concentration in the top membrane leaflet is ϕ while the lipid concentration in the bottom membrane leaflet is $-\phi$. The phenomenological energy of partially wrapping a bilayer membrane about an object is given by

$$E[C(\mathbf{S}),\phi(\mathbf{S})] = \oint d\mathbf{S}\left[\frac{\kappa}{2}\{C(\mathbf{S})-\bar{C}[\phi(\mathbf{S})]\}^2+\sigma-wg(\lambda)+\frac{\gamma}{2}|\nabla\phi|^2+f[\phi]\right]-\sigma A_T. \quad (1)$$

In Eq. (1), κ is the local membrane bending rigidity, σ is the surface tension, and w is the binding energy per unit area between the particle and the membrane. $C(\mathbf{S})$ is the local mean curvature at position $\mathbf{S}$ on the membrane surface, $\bar{C}[\phi(\mathbf{S})]$ is the spontaneous curvature generated by a local imbalance $\phi(\mathbf{S})$ between the concentrations of the two lipids, $f[\phi]$ is a local phenomenological free-energy functional of ϕ containing all contributions from excess concentrations, $\gamma|\nabla\phi|^2$ is a line tension contribution from surface gradients in ϕ, and A_T is the area of the membrane's projection on the horizontal plane. The σA_T term in Eq. (1) shifts E such that the energy of a flat membrane with no particle bound is defined to be zero. The Lagrange multiplier λ, which vanishes on the free, unattached membrane, is used to constrain the bound part of the membrane to the surface of the particle. The function $g(\lambda)$ is an indicator function that is unity within the contact region (where $\lambda\neq 0$) and zero where the membrane is unattached (where $\lambda=0$). Although we present our derivations in terms of a membrane wrapping a solid object, clathrin-mediated endocytosis is also described by our model if clathrin-coated regions of the membrane are treated as

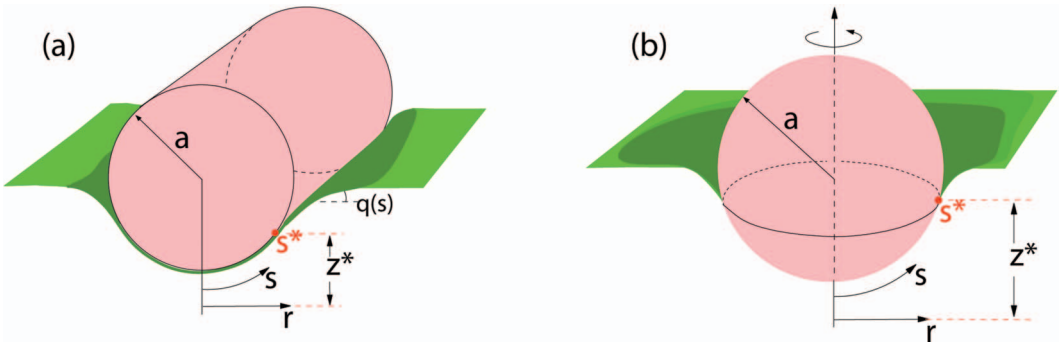

FIG. 2. (Color) (a) Membrane wrapping of a cylindrical particle of radius a. Here, s is the arclength from "south pole" of the particle to a point on the membrane, $q(s)$ is the angle that the membrane at position s makes with the horizontal, and s^* is the point where the membrane detaches from the particle. The horizontal distance from the midline is r, and the height of the membrane from the south pole is z. (b) Membrane wrapping of a spherical particle of radius a.

though they were bound to a solid sphere. The growing pit corresponds to progressive wrapping of the membrane and the binding energy per area, w, can be defined as the interaction energy per unit area between the clathrin and the membrane.

The most convenient mathematical representation of the total free-energy density and the surface element $d\mathbf{S}$ depends on the geometry being studied. If membrane deformation is sufficiently small such that there are no "overhangs," the Monge gauge can be used to derive a fourth-order partial differential equation describing the variations in height [44]. These equations can be linearized in the small distortion limit to find explicit analytical expressions for the surface height. In axisymmetric systems, extremization of E with respect to $C(\mathbf{S})$ and $\phi(\mathbf{S})$ leads to a second-order nonlinear ordinary differential equation involving the local mean and Gaussian curvatures [45] and two-point boundary values.

In this work, we extend the Hamiltonian approach used in [18] and described in [46]. Since we restrict our study to two-dimensional and axisymmetric geometries, we can find an energy density that depends on a single spatial variable. A set of nonlinear, coupled, first-order ordinary differential equations, with associated boundary conditions, can be derived from the total energy density (Appendix A). The resulting boundary value problem can be solved using a shooting method [18] or by using a two-point boundary value solver in a large domain. In Sec. III, we use a two-point boundary solver that employs a relaxation method, giving better efficiency than shooting methods.

A. Cylindrical particles

In this section, we explicitly derive equations that describe a membrane wrapping around an infinite cylinder of radius a lying with its axis parallel to the membrane. We define $q(s)$ as the local angle that the membrane makes with the $\hat{\mathbf{x}}$ axis, where s is the surface coordinate, measured from the lowest point of contact ("south pole") in the axisymmetric system [see Fig. 2(a)]. Upon introducing the notation $Y'(s) \equiv \partial_s Y(s)$ and recognizing that $q'(s)=C(s)$, Eq. (1) becomes $E=2\ell\int_0^\infty \mathcal{L}(q,q',\phi,\phi')ds$ for a segment of length ℓ of an infinite cylinder where

$$\mathcal{L}(q,q',\phi,\phi',\lambda) = \frac{\kappa}{2}(q'-\alpha\phi)^2 + \sigma(1-\cos q) + \frac{\gamma}{2}\phi'^2 + f[\phi] - wg(\lambda) - \lambda(q'-1/a) \tag{2}$$

is the free-energy density. Here, $\alpha\phi$ is the local spontaneous mean membrane curvature induced by local excess of either lipid type. Physically, α is a measure of how conical the lipids are. For "cylindrical" lipids, which induce no spontaneous curvature in the membrane, $\alpha=0$. The $\sigma\cos q$ term, which for a flat membrane integrates to σA_T, sets the energy of a flat membrane to zero, serving the same purpose as the σA_T term in Eq. (1). The functional $f[\phi]$ represents the enthalpy and free energy of mixing associated with the surface concentration ϕ and will be approximated with a Landau expansion with coefficients c_i and chemical potential μ:

$$f[\phi(s)] = \frac{c_2}{2!}\phi^2 + \frac{c_3}{3!}\phi^3 + \frac{c_4}{4!}\phi^4 + \cdots - \mu\phi. \tag{3}$$

Upon defining the dimensionless surface coordinate $S \equiv s/a$, the dimensionless length $L=\ell/a$, and the dimensionless quantities

$$\Gamma = \frac{2\gamma}{\alpha^2 a^2 \kappa}, \quad \Sigma = \frac{2a^2\sigma}{\kappa}, \quad \Phi = a\alpha\phi,$$

$$W = \frac{2a^2 w}{\kappa}, \quad C_i = \frac{2c_i}{\kappa\alpha^i a^{i-2}}, \quad \tilde{\mu} = \frac{2a\mu}{\alpha\kappa}, \quad \Lambda = \frac{2a\lambda}{\kappa}$$

$$\tilde{\mathcal{L}} = \frac{2a^2}{\kappa}\mathcal{L}, \quad \tilde{E} = \frac{E}{\kappa}, \tag{4}$$

we can write

$$\tilde{\mathcal{L}} = (q'-\Phi)^2 + \Sigma(1-\cos q) + \frac{\Gamma}{2}\Phi'^2 + f[\Phi] - Wg(\Lambda) - \Lambda(q'-1) \tag{5}$$

and $\tilde{E}=2L\int_0^\infty \tilde{\mathcal{L}}\, dS$, where

$$f[\Phi(S)] = \frac{C_2}{2!}\Phi^2 + \frac{C_3}{3!}\Phi^3 + \frac{C_4}{4!}\Phi^4 + \cdots - \tilde{\mu}\Phi. \tag{6}$$

From the Lagrangian [Eq. (5)], we use Hamiltonian approach [46] to derive a set of coupled, first-order differential equations, with associated boundary conditions in Appendix A. We solve these equations [Eqs. (A3) and (A4)] separately in the bound and unbound regions, and match the solutions at the point of membrane detachment S^* (also to be determined). By expressing the Lagrangian in a form that is valid in both the region where the membrane is bound and the region where the membrane is unbound, we can derive the conditions on the detachment point S^* that are necessary for an extremal solution. The value of S^* that minimizes the system's free energy simultaneously satisfies the conditions on the detachment point and the boundary conditions. For the membrane energy to be finite, the angle variable $q(s)$ must be continuous everywhere. The variables Φ and Φ' are also continuous. The mean membrane curvature q' is not continuous, and the jump condition

$$\lim_{\varepsilon\to 0}[q'(S^*+\varepsilon)-q'(S^*-\varepsilon)]=-\sqrt{W} \tag{7}$$

is derived in Appendix B. The continuity of the other variables is discussed here as well. For a more general derivation and a discussion of contact line conditions, see Ref. [47]. Since closed-form analytic solutions to the Euler-Lagrange equations (A1) and (A2) derived in Appendix A cannot be found, we present results of asymptotic and numeric analysis in Appendix A and in Sec. III.

B. Spherical particles

Here, we derive equations describing the membrane as it binds axisymmetrically to a spherical particle in the presence of curvature-inducing lipids. This geometry is appropriate for modeling the endo- and exocytosis of spherical virus particles and the binding of a spherical protein scaffold, such a clathrin, to the cell membrane. The profile of a membrane wrapping an infinite cylinder can be completely parametrized by the arc length s and the angular orientation of the membrane, $q(s)$. However, for a spherical particle, we must introduce an additional coordinate $r(s)$, the radial distance from the vertical axis of the sphere to the curve s [cf. Fig. 2(b)]. We define z^* to be the engulfment depth, or the vertical distance from the south pole of the sphere to the detachment point, s^*. For a membrane bound sphere, the energy is $E=2\pi\int_0^\infty \mathcal{L}\,ds$, where the density is given by

$$\mathcal{L}(q,q',\phi,\phi',r',r)=r\left[\frac{\kappa}{2}\left(q'+\frac{\sin q}{r}-\alpha\phi\right)^2+\sigma(1-\cos q)+f[\phi]+\frac{\gamma}{2}\phi'^2-wg(\lambda_q)\right]+\lambda_r(r'-\cos q)+\lambda_q(q'-1/a), \tag{8}$$

which, upon introducing the dimensionless quantities $R=r/a$ and

$$W=\frac{2a^2w}{\kappa},\quad C_i=\frac{2c_i}{\kappa a^{i-2}\alpha^i},\quad \tilde{\mu}=\frac{2a\mu}{\alpha\kappa},\quad \Lambda_R=\frac{2a\lambda_r}{\kappa}, \tag{9}$$

becomes

$$\tilde{\mathcal{L}}(q,q',\Phi,\Phi',R,R')=R\left[\left(q'+\frac{\sin q}{R}-\Phi\right)^2+\Sigma(1-\cos q)+f[\Phi]+\frac{\Gamma}{2}\Phi'^2-Wg(\Lambda_q)\right]+\Lambda_R(R'-\cos q)+\Lambda_q(q'-1). \tag{10}$$

With the definition $\tilde{\mathcal{L}}=\frac{2a}{\kappa}\mathcal{L}$, the dimensionless energy $\tilde{E}=\frac{E}{\kappa\pi}=\int_0^\infty \tilde{\mathcal{L}}\,dS$. At the detachment point S^*, we have the following jump condition on $q'(S)$:

$$\lim_{\varepsilon\to 0}=[q'(S^*+\varepsilon)-q'(S^*-\varepsilon)]=-\sqrt{W}, \tag{11}$$

identical to Eq. (7) from the case of a cylindrical particle (see Appendix B). As in the cylindrical case, no closed-form analytic solutions to the Euler-Lagrange equations (A27) can be found and we analyze the problem using asymptotic and numeric methods in the following sections.

III. RESULTS

Here, we present analytic and numeric results for large and small coupling strengths α. We show that the coupling strength modulates lipid segregation. The order parameter describing the strength of lipid segregation, Φ, affects the total free energy of the lipid membrane through two competing terms. On the one hand, the Helfrich part of the free energy decreases as Φ approaches the local mean curvature. On the other hand, when there is no phase transition, the Landau free energy $f[\Phi]$ increases as the lipids segregate. In the weak coupling limit, where we identify ε with α, the Landau free energy influences local lipid concentration more strongly than the Helfrich free energy and the lipids only weakly segregate. In the strong curvature-concentration coupling limit, where $\varepsilon\sim 1/\alpha$, the Helfrich free energy affects local lipid concentrations more strongly than the Landau free energy or the line-tension term and large local excesses of either lipid can induce large spontaneous curvatures. Results are derived by assuming that all dependent variables Y can be expanded in a series

$$Y=Y_0+\xi Y_1+\xi^2 Y_2+\cdots, \tag{12}$$

where

$$\xi=\varepsilon^\eta \tag{13}$$

and η is some power depending on whether we are expanding about the weak or strong coupling limits. Asymptotic formulas are derived for both cylindrical and spherical particles in each limit.

A. Weak coupling

In the limit $\alpha\sim\varepsilon\ll 1$, our problem reduces to that of a single-component membrane wrapping a colloid. In this

limit, the nondimensionalization relations [Eqs. (4) and (9)] imply $\Gamma \sim C_2 \sim \varepsilon^{-2} \gg 1$. The Landau free energy $f[\Phi]$ and the line tension $\frac{\Gamma}{2}\Phi'^2$ therefore affect local lipid concentrations more strongly than the Helfrich free energy, and lipids A and B segregate little. In this limit, $\Phi \sim O(\varepsilon^2)$ and the Landau free energy and the line tension are both $O(\varepsilon^2)$ and may be neglected. The binary mixture only weakly affects the mechanics of adhesion-mediated wrapping in this limit. Previous studies have considered a single-component membrane wrapping a sphere using the present approach [18], and the results presented here are consistent with those results.

First, take the wrapped particle to be a long cylinder. To lowest order in $\varepsilon \sim \alpha$, $\Phi = 0$ and the shape of the membrane determined from Eqs. (A3), (A12), and (A14) in Appendix A is

$$q_0(S) = \pm 4 \arctan e^{-\sqrt{\Sigma/2}S + C}. \tag{14}$$

This result was also presented in [48]. The first-order correction to $q(S)$ due to the lipid segregation is $O(\varepsilon^2) \sim O(\alpha^2)$.

To lowest order, the detachment point S^* is given by

$$q_0(S^*) = \arccos\left[1 - \frac{(1-\sqrt{W})^2}{\Sigma}\right], \tag{15}$$

which determines the integration constant

$$C = \ln\left(\frac{\sqrt{2} \mp \sqrt{1+q_0(S^*)}}{\sqrt{1-q_0(S^*)}}\right) - \sqrt{\frac{\Sigma}{2}} q_0(S^*). \tag{16}$$

Equation (15) is valid only for $W \geqslant 1$. For binding energies W less than unity, the cost of bending the membrane around the particle is too large for wrapping to be energetically favorable. Therefore, the particle will be unwrapped when $W \leqslant 1$ and will begin to be partially wrapped when $W > 1$. Thus, the curve $W=1$ defines the boundary between the region of phase space where the particle is unwrapped and where it is partially wrapped. While we might want to find the boundary between the partially wrapped and fully wrapped states from Eq. (15) by setting $q(S^*) = \pi$, this is not appropriate since Eq. (14) does not always yield physical solutions. We have not explicitly included potentials or forces by which the membrane interacts with itself; consequently, some solutions result in "phantom membranes"—i.e., calculated curves that pass through themselves if $R(S)$ [the membrane's x coordinate at S; see Fig. 2(a)] becomes negative. One such intersecting curve is shown in Fig. 3(a).

In Appendix A, we derive an expression for when the particle is *just* fully wrapped as shown in Fig. 3(b), and this curve is used to determine the boundary between the partially and fully wrapped states. In total, there are three phases for a membrane wrapping a cylindrical particle. The particle may be unwrapped, partly wrapped, or fully wrapped. The phase diagram for this system is shown in Fig. 3(c). Also shown in Fig. 3(c) is the shift in the phase diagram (dashed curve) when the concentration-curvature coupling α is strong, which is studied in the next subsection.

Now consider the small-α limit for membrane wrapping around a sphere. To first order, the equations found in this limit (derived in Appendix A) are equivalent to those used in

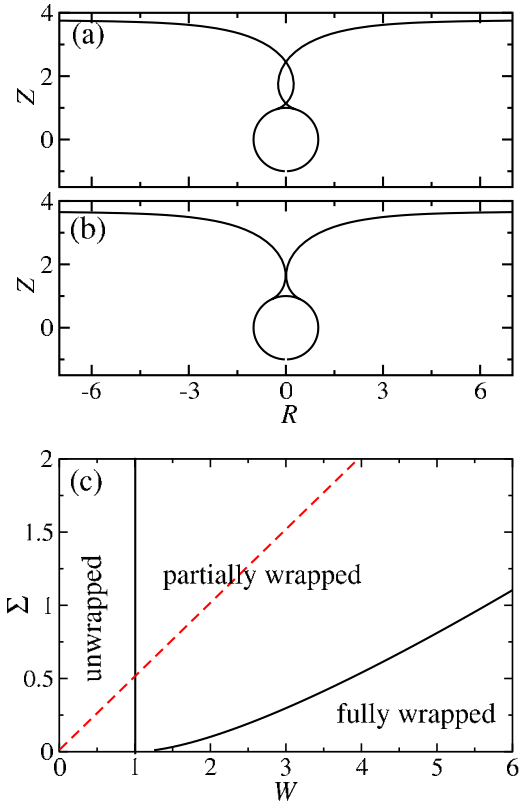

FIG. 3. (Color online) Wrapping of cylindrical particles. (a) For certain values of W and Σ (here, $\Sigma=1$, $W=5.81$), the solution is unphysical because the membrane curve crosses itself. (b) The solution curve for a particle that is just fully wrapped is plotted. The parameters $\Sigma=1$ and $W=5.65$ [which were calculated using Eq. (A20)] were used. (c) There are three possible phases for a cylindrical particle in the weak coupling limit (delineated by solid curves) describing particles that are unwrapped (when $W<1$), partially wrapped, or fully wrapped. The boundary between the partially wrapped and fully wrapped phases was found numerically using Eq. (A20). In the strong coupling limit ($\alpha \to \infty$), only two phases survive as shown by the dashed curve. For parameter values that lie above the dotted curve, we expect the particle to be partly wrapped; for parameters below the curve, the particle will be fully wrapped. Compared to the weak coupling limit, wrapping is enhanced by lipid segregation when the coupling α increases.

[18]. In contrast to the cylindrical case where, in some solutions, the membrane nonphysically intersects with itself, in the spherical case, the bending energy $R(q' + \frac{\sin q}{R} - \Phi)$ diverges as $R \to 0$, effectively creating a diverging barrier at the origin though which the membrane cannot pass.

For spherical wrapping, we find the four qualitatively different regimes, or "phases," discussed in [18]. In phase I, only the completely unwrapped state is energetically stable. As we increase the binding energy W, a stable fully wrapped state emerges in phase II [cf. Figs. 4(a) and 4(b)]. The stable state arises because surface tension provides an effective line tension that encourages wrapping near the fully wrapped state. The binding energy per unit area, W, also encourages wrapping. On the other hand, the bending energy (which is equal to 4 in our nondimensionalization) makes wrapping energetically unfavorable. Very roughly, the transition be-

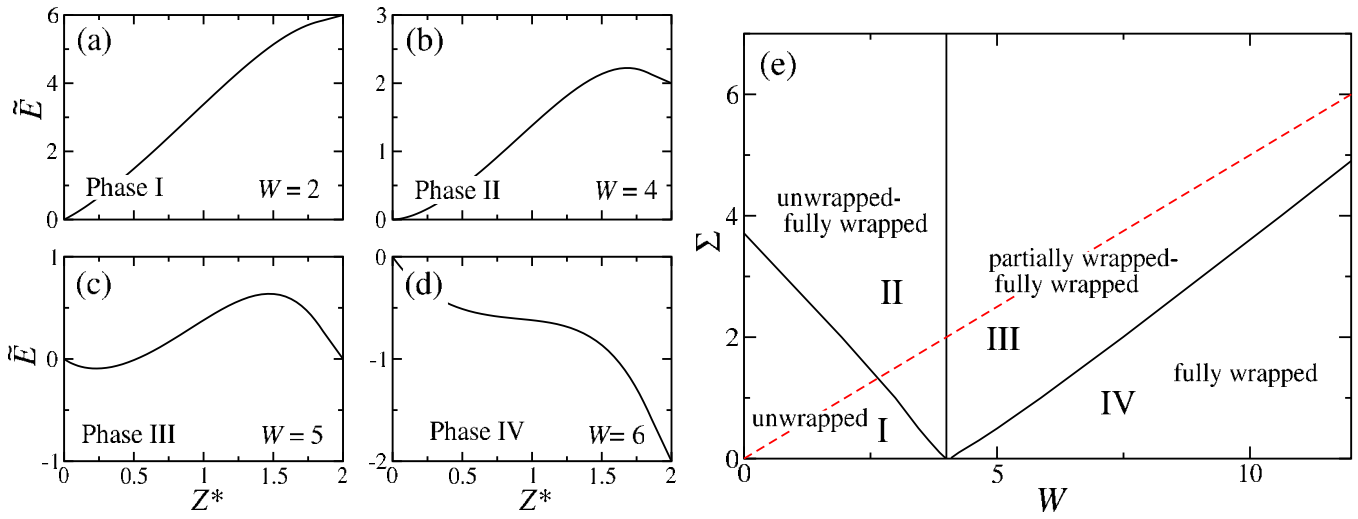

FIG. 4. (Color online) Wrapping of spherical particles. (a)–(d) The total energy of a membrane bound to a spherical particle is plotted as a function of $Z^*=z^*/a$. Surface tension was set to $\Sigma=1$, and the binding energy W was varied. (a) In the first phase, the binding energy is very low, and energy increases monotonically with Z^*. (b) At higher binding energies, an unstable equilibrium emerges, and both the fully wrapped state and the unwrapped state are energetically stable. (c) As W increases further, a stable equilibrium emerges as the unbound state becomes unstable. (d) When W is sufficiently large, the system is driven towards a fully wrapped state. (e) Phase diagram for spherical particles with no curvature coupling (solid curves) were determined numerically. The dashed curve shows the boundary between the two phases—partial wrapping and full wrapping—that occur in the limit where coupling α between concentration and spontaneous curvature is very large. Above the dashed curve, the particles are partly wrapped; below, they are fully wrapped. Strong coupling enhances wrapping.

tween phases I and II in the W-Σ phase diagram shows where surface tension and binding balance bending. It is not too surprising then that this transition curve looks qualitatively like $\Sigma+W\approx 4$.

Figure 4(b) shows that in the second phase a stable unwrapped and a stable fully wrapped state coexist, with a potentially sizable energy barrier between the two states. In this phase, the energy of the unwrapped state will always be zero, while the energy of the fully wrapped state will be $2(4-W+\Sigma)$ [18]. We will soon show that the boundary between regions II and III occurs at $W=4$; thus, the energy of the fully wrapped state in region II is always positive.

As discussed in [18], at $W\gtrsim 4$, the unwrapped state becomes unstable and a stable partially wrapped state emerges. For small binding levels ($Z^*\approx 0$), the membrane binds to the colloid at the expense of only the bending energy. Everywhere on the sphere, the mean curvature is 2 and the dimensionless energy per unit area attributable to bending is 4. The stable fully wrapped state remains and, in phase III, there are two stable states: a partially wrapped state and a fully wrapped state [cf. Fig. 4(c)].

Finally, as we increase W, the stable partially wrapped state and the unstable state at the maximum of the energy barrier annihilate each other at a saddle node, and the system is driven towards the fully wrapped state [cf. Fig. 4(d)]. Roughly, for there to be a single equilibrium point at $Z^*=2$, W must dominate the combined effects of surface tension and bending energy. The curve that defines the boundary between phases III and IV, therefore, shows where the surface tension and bending energy balance the binding energy. This transition line is approximated by $W\approx\Sigma+4$. A complete phase diagram for the wrapping of a spherical particle when $\alpha=0$ is shown by the solid curves in Fig. 4(e). For the strong coupling limit, we will now see that the phase diagram is modified (dashed curve) where only partially and fully wrapped states can arise, similar to the cylindrical case.

B. Strong coupling

In this section, we consider the strong coupling limit where $\alpha\sim 1/\varepsilon$. In this large-α limit, Eqs. (4) and (9) imply $\Gamma\sim C_2\sim\varepsilon^2$. Because the energetic and entropic cost of segregating lipids, $f[\Phi]$ and $\frac{\Gamma}{2}\Phi'^2$, becomes small, the lipids segregate in such a way that the spontaneous curvature $\bar{C}=\Phi$ approximates the local mean curvature everywhere, causing the Helfrich free energy to become small. Thus, surface tension and membrane-particle adhesion are the dominant energies.

First consider a membrane binding to an infinite cylindrical particle. Upon expanding all variables according to Eq. (12), to lowest order, the membrane shape is governed by

$$\frac{1}{\xi^4}\Gamma q_0'''' = -\Sigma \sin q_0, \tag{17}$$

as shown in Appendix A. The left-hand side of Eq. (17) scales as $O(\varepsilon^2/\xi^4)$, while the right scales as $O(1)$. We conclude that $\varepsilon\sim\xi^2$ and that the width of the boundary layer (and the radius of curvature with which the membrane bends at the point of detachment) scales as $\sqrt{\varepsilon}\sim\alpha^{-1/2}$. There is also a boundary layer in Φ within the bound region at $S\lesssim S^*$. The width of this boundary layer scales as $\varepsilon\sim\alpha^{-1}$. The concentration Φ in the region of the membrane bound to a cylindrical particle was calculated in Appendix A, and the width of the boundary layer can be calculated from Eq. (A9).

Although Eq. (17) does not admit a simple analytic solution, we can determine S^* in the limit of very large α. In this

limit, the energetic cost of segregating the lipids (parametrized by Γ and C_2) is small relative to all other energies in the problem. It costs little to induce a spontaneous curvature in the membrane, so the spontaneous curvature will be nearly equal to the mean curvature everywhere. The surface tension Σ and the binding constant W dominate. We can further assume that the energetic contribution of the free membrane is negligible. The free membrane is flat except in a region of width $\alpha^{-1/2}$. We show in Appendix A that within the boundary layer, $(q'-\Phi)\sim O(1)$. In this region, the surface-tension, Helfrich-free-energy, and line-tension contributions to the Lagrangian are all $O(1)$; the Landau free energy is $O(\varepsilon)$. Thus, the energy highly curved boundary layer is $O(\varepsilon)$. Upon using Eq. (2) to find an expression for the energy of the system in the limit of large α,

$$\tilde{E}(S^*) \approx \int_0^\infty \tilde{\mathcal{L}}(q,q',\Phi,\Phi')dS \approx \int_0^{S^*} \{\Sigma[1-\cos q_0(S)]-W\}dS. \tag{18}$$

The value of S^* that minimizes $\tilde{E}(S^*)$ must satisfy

$$d\tilde{E} \approx \{\Sigma[1-\cos q_0(S^*)]-W\}dS = 0. \tag{19}$$

Thus,

$$q_0(S^*) \approx \cos^{-1}\left(1-\frac{W}{\Sigma}\right). \tag{20}$$

Note that this is simply the Young-Dupré equation: the condition on the contact angle of a membrane with surface tension but no bending energy. Strong coupling between Φ and spontaneous membrane curvature effectively removes bending energy from the Hamiltonian, and the boundary condition at S^* is described by the Young-Dupré equation. Setting $q(S^*)=\pi$, we can determine when the particle is fully wrapped in the strong coupling limit. The result $W=2\Sigma$ is plotted (dashed line) in Fig. 3(c) and represents the boundary between the partly wrapped and fully wrapped phases. From Fig. 3(c) and comparing Eqs. (15) and (20), it is evident that a membrane with lipids that strongly induce curvature will always wrap a colloid more than a single-component membrane.

Finally, consider a membrane wrapping a spherical particle in the large-α limit. As we found in the previous section, the cost of bending the membrane is low when the coupling constant α is large. Assuming that the membrane bends with radius of curvature $\xi \ll 1$ near the detachment point, to first order,

$$\frac{1}{\xi^4}\Gamma q_0'''' = -\Sigma \sin q_0, \tag{21}$$

which is derived in Appendix A. Note that Eq. (21) is identical to Eq. (17). In the presence of strong coupling between Φ and the mean curvature, the bending energy becomes unimportant, and the sphere's azimuthal curvature does not affect the membrane's mechanics. In fact, in the large-α limit, from Eq. (10), the energy of the system is

$$\tilde{E} = \int_0^\infty \tilde{\mathcal{L}}(q,q',\Phi,\Phi',R,R')dS \approx \int_0^{S^*} R_0[\Sigma(1-\cos q_0)-W]dS. \tag{22}$$

Equation (22) parallels Eq. (18), so for $\alpha \gg 1$, the detachment point that minimizes the spherical system energy also obeys the Young-Dupré equation $q_0(S^*)=\cos^{-1}(1-W/\Sigma)$ given by Eq. (20). The differential equation describing the membrane shape is identical for a membrane wrapping spherical and cylindrical particles, and the boundary conditions are also the same. Thus, the ultimate membrane shape defined by $q(S)$ is, to first order, the same in the cylindrical and spherical cases. When $\alpha \gg 1$, the lipids segregate freely and the spontaneous curvature will nearly equal the mean curvature. The cost of bending the membrane effectively disappears. As shown in Sec. III A, the boundary between phases II and III (Fig. 4) occurs when the binding energy just equals the bending energy demanded by the sphere's curvature. When α is small, the boundary between phases II and III occurs at $W=4$. Because we can neglect the energetic cost of bending the membrane when α is very large, the boundary between phases II and III moves to $W=0$. As in the cylindrical geometry, the boundary between the partially wrapped and fully wrapped phases is given by $W=2\Sigma$ and is plotted in Fig. 4(e) (dashed line). Comparing the phase diagrams found in the small- and large-α limits, it is evident that large coupling between lipid concentration and spontaneous curvature not only enhances membrane-particle wrapping, but also destroys all unwrapped phases.

Using the MATLAB boundary problem solver BVP4C [49], we numerically solve for the membrane profiles and lipid concentrations. We find that as we increase α, a weaker binding interaction (smaller W) is sufficient to wrap a particle a specified amount [see Fig. 5(a)]. For relatively large $\alpha \gg 1$, $\Phi \approx 2$ in the bound region (to match the mean curvature); Φ decreases rapidly across the detachment point to generate a large negative curvature to sharply bend the membrane to horizontal. Far from the particle, Φ relaxes back to zero. The effect of α on Φ is shown in Fig. 5(b).

IV. DISCUSSION

In the preceding analysis, we ignored all terms third order or higher in $f[\Phi]$. In this section, we will discuss the conditions under which we expect the approximation $f[\phi] \approx \frac{c_2}{2}\phi^2$ to be valid. We will see that if there is a local minimum in $f[\phi]$ at $\phi=0$, ϕ will be small in both the $\alpha \ll 1$ and $\alpha \gg 1$ limits. All quantities scale similarly in the cylindrical and spherical cases, so we will refer to examples from the cylindrical case for simplicity. In Sec. III A, we found that when $\alpha \ll 1$, $\Phi \sim \alpha^2$; therefore, by Eqs. (4), $\phi \sim \alpha$. Thus, the dimensional order parameter ϕ is small and $f[\phi]$ should be well approximated by a quadratic function.

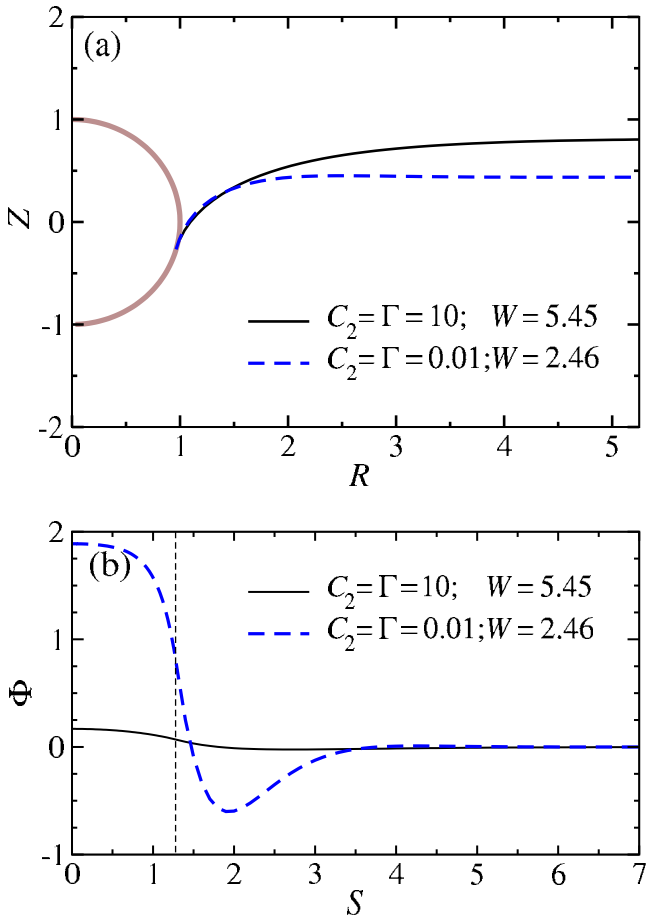

FIG. 5. (Color online) Membrane shapes and concentration profiles for a partially wrapped sphere. (a) The profile of two free membranes are plotted. The detachment point $S^*=1.3$ was fixed. With increased coupling constant α (and decreased C_2 and Γ), the membrane bends more sharply at the detachment point and becomes flat more quickly. The binding energy necessary to wrap the specified amount was calculated and is significantly lower for larger α (W=2.46 vs 5.45). In (b), $\Phi(S)$ is plotted for the two profiles shown in (a). With increased α (and decreased C_2, Γ), Φ and Φ' reach larger values. The dashed line marks the point at which the membrane detaches from the sphere.

When the coupling between concentration and curvature is strong ($\alpha\sim 1/\varepsilon \gg 1$), $\Phi\sim\sqrt{\alpha}$ within the region (of width $\sqrt{\varepsilon}$) with the sharpest curvature [Eq. (17)]. This means that $\phi\sim\frac{1}{\sqrt{\alpha}}\sim\sqrt{\varepsilon}$. It is somewhat counterintuitive that ϕ should be small in a region where the mean membrane curvature is large and the mean curvature is strongly coupled to ϕ. From Eq. (17), it is evident that the surface tension and the line tension $\frac{\gamma}{2}(\phi')^2$ ultimately balance. Because surface tension is $O(1)$, ϕ' is necessarily $O(1)$ and $\phi\sim\sqrt{\varepsilon}$. Therefore, in the strong coupling limit, $\frac{\gamma}{2}(\phi')^2$ dominates $f[\phi]$; consequently, $\phi\ll 1$ and the quadratic approximation of $f[\phi]$ is also good in the strong coupling limit. Moreover, in the strong coupling limit, the solution will not depend strongly on the exact form of $f[\phi]$ as the equation governing the membrane shape, Eq. (17), is independent of $f[\phi]$.

In either extreme $\alpha\gg 1$ or $\alpha\ll 1$, a local minimum in $f[\phi]$ can be approximated by a quadratic function in ϕ about the minimum ϕ_0. If we make the change of variables $\tilde{\phi}=\phi-\phi_0$, it is straightforward to show that the shape [Eqs. (A3) and (A4)] are recovered. Higher-order terms may be required in order to accurately describe the system when $\alpha\sim O(1)$.

We will now discuss the relevance of phase separation. If the system is at a temperature well below that of phase separation, we assume that there are two local minima in the Landau free energy $f[\Phi]$ at concentrations Φ_1 and Φ_2. Suppose $|\Phi_1|<|\Phi_2|$ and $f[\Phi_1]\approx f[\Phi_2]$. Then, if $|\Phi_2-2|<|\Phi_1-2|$, $\Phi\approx\Phi_2$ in the bound region and $\Phi\approx\Phi_1$ in the unbound region. Suppose that the domain wall between the A-rich and B-rich phases is of width δ such that we can approximate the line tension energy by $\Gamma(\frac{\Phi_2-\Phi_1}{\delta})^2$. If the particle is nearly fully wrapped, the energy of the system is approximately $\tilde{E}\approx\tilde{E}_F-R^2h_1[\Sigma,W,\Phi_1]+Rh_2[\Gamma,\Phi_1,\Phi_2,\delta]$, where $\tilde{E}_F$ is the energy of a fully wrapped particle, R is the radial distance from the contact point to the origin, h_1 is the effective energy per unit area of bound membrane near the fully wrapped state, and h_2 is some function describing the energy of the phase boundary. There will be a stable fully wrapped state provided $-\frac{\partial E}{\partial R}<0$, and the system energy decreases as the particle becomes fully wrapped (and R decreases). This will always be the case for $R\ll 1$ as the energetic contribution from the line-tension term will dominate in the limit of small R. In strongly phase-separated regimes the configuration in which there is only a stable unwrapped state (phase I) disappears, and even for very small binding energies, there is a stable fully wrapped state. The formation of vesicles by only a phase separation line tension and without any binding interactions has been studied in [32].

Finally, as seen in Fig. 1(b), long membrane necks are sometimes observed during endocytosis. The model presented, even with two-component lipid segregation, yields typically spherically shaped wrapping configurations and cannot account for extended membrane necks. Since long necks imply larger regions of negative Gaussian curvature, we briefly consider coupling between local concentration Φ and Gaussian bending rigidity κ_G in the spherical case. Here, we consider a κ_G that varies continuously. Budding of a two-component membrane in which each component has a different Gaussian bending rigidity has been studied [31,50,51]. An appreciable κ_G (relative to κ) has been suggested by recent simulations of protein-embedded lipid bilayers [34]. A Lagrangian that includes coupling between κ_G and Φ takes the form

$$\tilde{\mathcal{L}}=R\left[\left(q'+\frac{\sin q}{R}\right)^2+\Sigma(1-\cos q)+f[\Phi]+\kappa_G[\Phi]q'\frac{\sin q}{R}-Wg(\Lambda_q)\right]+\Lambda_R(R'-\cos q)+\Lambda_q(q'-1), \tag{23}$$

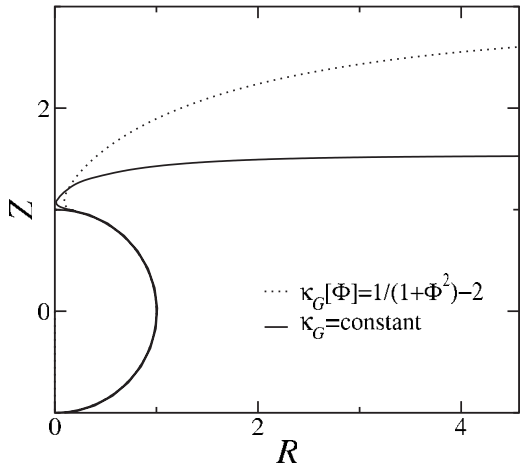

FIG. 6. Membrane shapes near full wrapping. The parameters $\Sigma=1$ and a detachment point at $q(S^*)=3$ (to approximate full wrapping) were used. Notice that when κ_G is variable, the relaxation of the membrane to a flat surface is more gradual and the region with negative Gaussian curvature is extended.

The integral of the Gaussian curvature $q'\frac{\sin q}{R}$ over the domain equals zero when the membrane has no deformation, and because the integral is a topological constant, it must always equal zero. If κ_G is not constant, the system could lower its free energy if

$$\int_{S^+} \kappa_G[\Phi] q' \frac{\sin q}{R} < \int_{S^-} \kappa_G[\Phi] q' \frac{\sin q}{R}, \tag{24}$$

where $\mathbf{S}^+$ is the region with positive Gaussian curvature and $\mathbf{S}^-$ is the region with negative Gaussian curvature. In our problem, the region of the membrane that is bound to the sphere has positive Gaussian curvature, while the region comprising the "neck" has negative Gaussian curvature. A simple model for concentration-dependent κ_G can be illustrated with the form $\kappa_G=(1+\Phi^2)^{-1}-2$, which allows κ_G to vary between -2 and -1. In the bound region, Φ is nonzero, which lowers $\kappa_G[\Phi]$. To minimize the energetic contribution of Gaussian curvature, $\Phi\approx 0$ in the neck (this maximizes $\kappa_G[\Phi]$). The larger region of Gaussian curvature that we observe in Fig. 6 when Φ-dependent κ_G is included represents the distance it takes for Φ to relax to zero from its value in the bound region. Although we see slightly longer necks, we do not find tetherlike formation during wrapping and endocytosis, as seen in Fig. 1(b).

V. SUMMARY AND CONCLUSIONS

We studied the effect of a binary lipid membrane on the mechanics of wrapping a long cylindrical or spherical particle. In the case of long cylindrical particles, we found that for some parameters, the solution curve of the membrane was self-intersecting and unphysical. We found an implicit formula for when the particle is fully wrapped and found that in this state the membrane captures the particle and some extra fluid volume. This is not the case with spherical particles, where the fluid membrane contacts the particle for arbitrarily large degrees of wrapping. When coupling between the spontaneous curvature of the membrane and the lipids is large, wrapping is encouraged as the energetic cost of bending the membrane is effectively lowered. In the limit of very large coupling, we could analytically find the detachment point S^* in both the spherical and cylindrical cases. The detachment point, as well as the membrane profile, were the same in both geometries, given the same values of the surface tension Σ and binding strength W.

Using numeric and asymptotic methods, we studied the limits in which the coupling between the spontaneous curvature of the membrane and the lipid concentration was weak and strong. In the weak coupling limit, we found three phases of behavior for cylindrical particles: the particles can be unwrapped, partially wrapped, or fully wrapped. We found four possible types of behavior for spherical particles, consistent with the results of [18]. The particles could have a single stable unwrapped or fully wrapped state, or they could have two energetically stable states (fully wrapped and unwrapped, or fully wrapped and partially wrapped), with an energy barrier between the two states. When the coupling α is large, nonwrapped configurations are energetically excluded and wrapping is enhanced.

The ideas presented in our analysis can be directly applied to virus entry and budding. The typical values for cell membrane surface tension and bending rigidity are $\sigma\approx 0.006 k_BT$ nm^{-2} [3] and $\kappa=10-20k_BT$ [6], respectively. For wild-type HIV-1, a typical size is $a=50$ nm [52]. According to Eqs. (4) and (9), $\Sigma\approx 1.5-3\sim O(1)$. The assumption $\Sigma=1$ used in Fig. 4 is therefore physically reasonable. In Ref. [52], the authors estimate the HIV-1 virus-membrane binding energy w to be $w\approx(0.07-0.14)k_BT$ nm^{-2}, which means $W\approx 17.5-70\gg 4$, indicating that the virus particle is strongly driven to the fully wrapped state and in phase IV. However, a number of factors, from low receptor density to mutations in the virus or cell receptors, could lower the effective W, perhaps allowing the other three scenarios to arise. HIV-1, under most conditions, enters through fusion rather than endocytosis. Therefore, the conditions under which endocytosis is observed may enhance the propensity for membrane wrapping, in addition to decreasing the fusogenic properties of the receptor-spike complex (CD4 and coreceptor bound to gp41) [53].

Now consider the endocytotic entry of the human rhinovirus serotype 3 (HRV3), a form of the cold virus. HRV3 binds the membrane protein intracellular adhesion molecule-1 (ICAM-1), and the thermodynamics of soluble ICAM-1 binding to HRV3 have been studied. Since the free energy of binding is $(11-13)k_BT$ per complex formed [54] (with 60 binding sites on each virus) and the radius of HRV3 is $a=15$ nm, the corresponding dimensionless binding energy is $W\approx 5-13$. Because HRV3 is much smaller than of HIV the effective dimensionless surface tension is smaller than that of HIV and is $\Sigma\approx 0.1-0.2$. From Fig. 4, we can see that these parameters put wrapping of HRV3 in phase IV and the system has only one stable equilibrium point, which is at $Z^*=2$ (fully wrapped).

Virus budding can also be viewed in terms of an interplay between membrane mechanics and composition. Retroviruses bud by hijacking the cellular pathway normally used

for the formation of multivesicular bodies. While some 25 proteins have been identified that are required for vesicle formation and HIV-1 budding [55], how membrane curvature is generated in the process is not well understood. Originally, it was thought that interactions between membrane-associated Gag proteins provide the energy necessary for membrane deformation, but a number of genetic experiments have complicated this view by showing that disruption of domains of the Gag protein not involved in Gag-Gag interactions can abolish budding. Furthermore, the conical lipid LBPA, which carries intrinsic curvature, has been shown to promote the formation of multivesicle bodies (MVBs) *in vitro* and is thought to play a role in MVB formation [55] and virus budding.

Because the dimensionless energy $\tilde{E}$ for wrapping of spherical particles is measured in units of $\kappa\pi \approx (30-60)k_BT$, we expect that for some parameters thermal fluctuations in the degree of membrane wrapping might be substantial [see, e.g., Fig. 4(c)]. However, in the HIV example, the energy barrier between the partially wrapped and fully wrapped state is $(15-30)k_BT$. Therefore, we would not expect the particle to become fully wrapped except at exponentially long times. Rather, we expect that the particle would remain in the energetically stable partially wrapped state until fusion occurs. However, wrapping may be stochastic in the presence of curvature-inducing lipid. Because most of the energy barrier is attributable to membrane bending rather than to surface tension, the barrier may be significantly reduced by the presence of curvature-inducing lipids, which have intrinsic curvatures ranging from about -1 to 0.5 nm^{-1} [9]. For example, if a lipid inducing a curvature of 0.25 nm^{-1} were to cover 10% of the area of the membrane in the bound region, the bending energy would be reduced by $\sim 85\%$, and particle wrapping could be stochastic for moderate values of W. For larger values of W, lipids with intrinsic curvature will serve to facilitate wrapping even further, and we expect strongly deterministic behavior when W is large.

Finally, one of the goals of this study was to understand the qualitative effect of membrane heterogeneity on membrane shape. In particular, we were interested in whether a two-component lipid membrane could produce the membrane tethers sometimes observed during endocytosis [Fig. 1(b)]. Such structures do not arise in our two-component model, suggesting that more complicated mechanics involving perhaps active cytoskeletal processes [52] are required to achieve significantly nonspherical wrapping.

ACKNOWLEDGMENTS

This work was supported by the NSF (Grant No. DMS-0349195) and by the NIH (Grant No. K25AI058672). S.A.N. also acknowledges support from the NSF. Much of this work was performed during the program on cells and materials at IPAM.

APPENDIX A: EULER-LAGRANGE EQUATIONS AND ASYMPTOTICS

1. Cylinders

The momenta conjugate to the coordinates $q(S)$ and $\Phi(S)$ in a cylindrical geometry are

$$p_q = \frac{\partial \tilde{\mathcal{L}}}{\partial q'} = 2(q' - \Phi) - \Lambda,$$

$$p_\Phi = \frac{\partial \tilde{\mathcal{L}}}{\partial \Phi'} = \Gamma \Phi', \tag{A1}$$

where $\tilde{\mathcal{L}}$ is taken from Eq. (5). The remaining equations of motion derived from the Lagrangian are

$$p_q' = \frac{\partial \tilde{\mathcal{L}}}{\partial q} = \Sigma \sin q,$$

$$p_\Phi' = \frac{\partial \tilde{\mathcal{L}}}{\partial \Phi} = -2(q' - \Phi) + \frac{\partial f[\Phi]}{\partial \Phi}. \tag{A2}$$

Upon differentiating Eqs. (A1) with respect to S and equating the result to Eqs. (A2), we obtain the following second-order equations:

$$2(q'' - \Phi') = \Sigma \sin q + \Lambda', \tag{A3}$$

$$\Gamma \Phi'' = -2(q' - \Phi) + \frac{\partial f[\Phi]}{\partial \Phi}. \tag{A4}$$

Associated with these equations are two independent boundary conditions consistent with a flat surface far from the adsorbed particle. For simplicity, we assume that the concentrations of lipids A and B are equal far from the particle, implying

$$\lim_{S\to\infty} q(S) = \lim_{S\to\infty} \Phi(S) = 0. \tag{A5}$$

From symmetry, two additional independent conditions arise at $S=0$:

$$\lim_{S\to 0} \Phi'(S) = q(S) = 0. \tag{A6}$$

Thus, $q'(s)$ is bounded, and Eqs. (A1) and (A2) imply that Φ and Φ' are also continuous across S^*. Finally, Eqs. (A1) imply that if there is a discontinuity in Λ across the detachment point, in order for p_q to be continuous across the detachment point [as is implied by Eqs. (A2)], there will be a corresponding discontinuity in q'. Therefore, we need a jump condition for q' across the detachment point S^*. This additional condition

$$\lim_{\varepsilon\to 0^+} [q'(S^* + \varepsilon) - q'(S^* - \varepsilon)] = -\sqrt{W} \tag{A7}$$

is derived in Appendix B.

In general, Eqs. (A3) and (A4) must be solved numerically. However, for the special case where $f[\Phi] \approx \frac{C_2}{2}\Phi^2$, we can find an analytic solution for the lipid concentration where the cell membrane is bound to the particle. In this bound region, the membrane curvature $q'=1$ is fixed, and the dimensionless concentration field obeys

$$\Gamma \Phi'' = (2 + C_2)\Phi - 2. \tag{A8}$$

Upon solving Eq. (A8) subject to the boundary conditions given in Eqs. (A5) and (A6), we find

$$\Phi(S) = A \cosh \sqrt{\frac{C_2+2}{\Gamma}} S + \frac{2}{2+C_2}. \tag{A9}$$

In the unbound region $S > S^*$, Eqs. (A3) and (A4) cannot be solved in closed form and numeric and asymptotic approaches are taken.

a. Weak coupling. Continuing with the approximation $f[\Phi] \approx C_2\Phi^2/2$, we first take the weak coupling limit $\alpha \equiv \varepsilon \to 0$. In this weak coupling limit, Eqs. (4) imply that $C_2 \sim \Gamma \sim \varepsilon^{-2}$. To lowest order in ε, Eq. (A4) becomes

$$\Gamma \Phi_0'' = C_2 \Phi_0 \tag{A10}$$

in both the bound and unbound regions. Equation (A10) is solved by

$$\Phi_0(S) = A_1 e^{(\sqrt{C_2/\Gamma}S)} + A_2 e^{(-\sqrt{C_2/\Gamma}S)}. \tag{A11}$$

For Eq. (A11) to satisfy the boundary conditions [Eqs. (A5) and (A6)], $A_1 = A_2 = 0$. In the unbound region, where $\Lambda = 0$, Eq. (A3) becomes

$$q_0'' = \frac{\Sigma}{2} \sin q_0. \tag{A12}$$

Upon integrating the above equation, we find

$$\frac{1}{2}(q_0')^2 = \frac{\Sigma}{2}(1 - \cos q_0) \tag{A13}$$

and the solution

$$q_0(S) = \pm 4 \arctan e^{-\sqrt{\Sigma/2}S + C}. \tag{A14}$$

This result was also presented in [48]. From the jump condition on q' at S^* [Eq. (7)], we substitute $q'(S^*) = 1 - \sqrt{W}$ into Eq. (A13) to find

$$q_0(S^*) = \arccos\left[1 - \frac{(1-\sqrt{W})^2}{\Sigma}\right] \tag{A15}$$

and the integration constant

$$C = \ln\left(\frac{\sqrt{2} \mp \sqrt{1+q_0(S^*)}}{\sqrt{1-q_0(S^*)}}\right) - \sqrt{\frac{\Sigma}{2}} q_0(S^*). \tag{A16}$$

We now determine for what values of Σ and W the particle is *just* fully wrapped—that is, $\min_S R(S) = 0$ [see Fig. 3(b)]. The minimum of $R(S)$ satisfies $\frac{dR}{dS} = \cos q(S) = 0$, the only physical solution of which is $q(S) = \pi/2$. Thus, we require that for some S_{cr},

$$R(S_{cr}) = 0 \quad \text{and } q(S_{cr}) = \frac{\pi}{2}. \tag{A17}$$

Using the relation, $dR = \cos q(S) dS$, we have

$$R_0(S_{cr}) = \int_{S^*}^{S_{cr}} \cos q(S) dS + R(S^*) = 0. \tag{A18}$$

From Eq. (A13), $dS = \frac{dq}{\sqrt{2\Sigma}\sin(q/2)}$, so Eq. (A18) can also be written as

$$R(S_{cr}) = \frac{1}{\sqrt{2\Sigma}} \int_{q_0(S^*)}^{\pi/2} \frac{\cos q}{\sin(q/2)} dq + R_0(S^*) = 0, \tag{A19}$$

which leads to the relation

$$\sqrt{\frac{2}{\Sigma}}\left(\sqrt{2+2\cos q_0(S^*)} - \sqrt{2} + \ln\left[\sqrt{\frac{2}{1-\cos q_0(S^*)}} - \sqrt{\frac{1-\cos q_0(S^*)}{1+\cos q_0(S^*)}}\right] - \ln(\sqrt{2}-1)\right) + \sin q_0(S^*) = 0. \tag{A20}$$

Upon substituting $q_0(S^*)$ from Eq. (A15) into Eq. (A20) we find an approximate relationship between Σ and W that defines the boundary between the partially wrapped and fully wrapped phases. The phase diagram for the wrapping of cylindrical particles is shown in Fig. 3(c).

The effects of the first-order correction can be revealed by considering the next-order equation for Φ_1 [Eq. (A4)]

$$\xi \Gamma \Phi_1'' = -2q_0 + \xi C_2 \Phi_1. \tag{A21}$$

Since $q_0 \sim O(1)$, ξ is $O(\varepsilon^2)$ [$\eta = 2$ in Eq. (12)]. From Eq. (A3),

$$2(q_1'' - \Phi_1') = \Sigma q_1, \tag{A22}$$

and we conclude that the first-order correction to $q(S)$ due to the lipid segregation is $O(\varepsilon^2) \sim O(\alpha^2)$.

b. Strong coupling. Now consider the limit $\alpha \equiv \varepsilon^{-1} \to \infty$. This implies that $C_2 \sim \Gamma \sim \varepsilon^2$. From Eqs. (A3) and (A4), we find

$$q_0' = \Phi_0 \quad \text{and } \Sigma \sin q_0 = 0. \tag{A23}$$

The outer solution $q_0 = 0$ in the region $S \gg S^*$ corresponds to a flat membrane. We must match the $q_0 = 0$ outer solution to an inner solution in the region $S \gtrsim S^*$. This inner solution must be constructed to satisfy both the continuity of $q(S)$, and the jump in $q'(S)$ at S^*.

If we rescale our surface coordinate with $\hat{S} = S/\xi$, where $\xi \ll 1$, Eq. (A3) becomes

$$2\left(\frac{1}{\xi^2} q'' - \frac{1}{\xi} \Phi'\right) = \Sigma \sin q \tag{A24}$$

within the boundary layer. Since $\Sigma \sin q = O(1)$, Eq. (A24) implies

$$\frac{1}{\xi^2}q_0'' \approx \frac{1}{\xi}\Phi_0' \tag{A25}$$

and $\Phi \sim O(\xi^{-1})$. Differentiating Eq. (A4) and combining the result with Eqs. (A24) and (A25), we have

$$\frac{1}{\xi^4}\Gamma q_0'''' = -\Sigma \sin q_0. \tag{A26}$$

The left-hand side of Eq. (A26) scales as $O(\varepsilon^2/\xi^4)$ while the right scales as $O(1)$. We conclude that $\varepsilon \sim \xi^2$ and that the width of the boundary layer (and the radius of curvature with which the membrane bends at the point of detachment) scales as $\sqrt{\varepsilon} \sim \alpha^{-1/2}$. There is also a boundary layer in the bound region at $S \lesssim S^*$. The width of this boundary layer scales as $\varepsilon \sim \alpha^{-1}$, which can be shown from Eq. (A9).

2. Spheres

We derive equations of motion for a membrane bound to a sphere. The Lagrange density $\tilde{\mathcal{L}}$ is taken from Eq. (10). The resulting Euler-Lagrange equations are

$$P_q = \frac{\partial \tilde{\mathcal{L}}}{\partial q'} = 2R\left(q' + \frac{\sin q}{R} - \Phi\right),$$

$$P_q' = \frac{\partial \tilde{\mathcal{L}}}{\partial q} = P_q \frac{\cos q}{R} + R\Sigma \sin q + P_R \sin q,$$

$$P_\Phi = \frac{\partial \tilde{\mathcal{L}}}{\partial \Phi'} = R\Gamma\Phi', \quad P_\Phi' = \frac{\partial \tilde{\mathcal{L}}}{\partial \Phi} = -P_q + R\frac{df[\Phi]}{d\Phi},$$

$$P_R = \frac{\partial \tilde{\mathcal{L}}}{\partial R'} = \Lambda_R,$$

$$P_R' = \frac{\partial \tilde{\mathcal{L}}}{\partial R} = \frac{P_q^2}{4R^2} - \frac{P_q \sin q}{R^2} + \Sigma(1-\cos q) + f[\Phi] + \frac{P_\Phi^2}{2R^2\Gamma}, \tag{A27}$$

and the boundary conditions far from the particle and at $S=0$ are

$$\lim_{S\to\infty} q(S) = \lim_{S\to\infty} \Phi(S) = \lim_{S\to\infty} P_r(S) = 0 \tag{A28}$$

and

$$\lim_{S\to 0} \Phi'(S) = \lim_{S\to 0} q(S) = \lim_{S\to 0} R(S) = 0. \tag{A29}$$

a. Weak coupling. We now consider the limit $\alpha \equiv \varepsilon \to 0^+$. From Eq. (9), $C_2 \sim \Gamma \sim \varepsilon^{-2}$. Upon combining Eqs. (A27) for P_Φ and P_Φ', we find to lowest order in $\alpha \sim \varepsilon$, $\Gamma\Phi_0'' = RC_2\Phi_0$, which, when combined with the boundary conditions given by Eqs. (A28) and (A29), is solved by $\Phi_0 = 0$. The remaining lowest-order equations of Eq. (A27) are

$$P_q = \frac{\partial \tilde{\mathcal{L}}}{\partial q'} = 2R\left(q' + \frac{\sin q}{R}\right),$$

$$P_q' = \frac{\partial \tilde{\mathcal{L}}}{\partial q} = P_q \frac{\cos q}{R} + R\Sigma \sin q + P_R \sin q,$$

$$P_R = \frac{\partial \tilde{\mathcal{L}}}{\partial R'} = \Lambda_R, \quad P_R' = \frac{P_q^2}{4R^2} - \frac{P_q \sin q}{R^2} + \Sigma(1-\cos q), \tag{A30}$$

where all dependent variables above are taken to represent their zeroth-order functions. Equations Eq. (A30) are equivalent to those for the wrapping of a single-component lipid membrane [18].

b. Strong coupling. Now consider the limit $\alpha \equiv \varepsilon^{-1} \to \infty$ where we know from Eq. (9) that $C_2 \sim \Gamma \sim \varepsilon^2$. We assume that the membrane bends with radius of curvature $\xi \ll 1$ near the detachment point.

Upon making the change of variables, $S \to \xi\hat{S}$, the second equation in Eqs. (A27) becomes

$$\frac{1}{\xi^2}R_0\Gamma\Phi_0'' = -2R_0\left(\frac{1}{\xi}q_0' + \frac{\sin q_0}{R_0} - \Phi_0\right). \tag{A31}$$

Upon substituting $P_q = 2R(\frac{1}{\xi}q' + \frac{\sin q}{R} - \Phi)$, dividing through by R, and differentiating, we find, to lowest order,

$$\frac{1}{\xi^3}\Gamma\Phi''' = -\frac{1}{\xi}\left(\frac{P_q'}{R} - \frac{P_q}{R^2}\cos q\right) = -\Sigma \sin q - P_r/R. \tag{A32}$$

After some consideration, the scalings $\xi \sim \sqrt{\varepsilon}$, $P_q \sim P_R \sim O(\xi)$, and $P_q' \sim P_R' \sim O(1)$ are found to be self-consistent with this lowest-order approximation and lead to

$$\frac{1}{\xi^3}\Gamma\Phi_0''' = -\Sigma \sin q_0. \tag{A33}$$

Within the boundary layer, $\frac{1}{\xi}q_0' = \Phi_0$; thus,

$$\frac{1}{\xi^4}\Gamma q_0'''' = -\Sigma \sin q_0. \tag{A34}$$

APPENDIX B: CURVATURE JUMP CONDITION

The Hamiltonian corresponding to the Lagrangian $\mathcal{L}$ in the cylindrical problem is

$$\mathcal{H} = p_q q' + p_\Phi \Phi' - \tilde{\mathcal{L}} = q'^2 - \Phi^2 - \Sigma(1-\cos q) + \frac{\Gamma}{2}\Phi'^2 - f[\Phi] + Wg(\Lambda) - \Lambda q'. \tag{B1}$$

The Lagrangian does not depend explicitly on S; $\mathcal{H}$ is thus constant for all values of S. If we define the jump in any function $X(S)$ at the contact point S^* as

$$[X(S)]_{S^*} \equiv X_+ - X_- = \lim_{\varepsilon\to 0} X(S^*+\varepsilon) - \lim_{\varepsilon\to 0} X(S^*-\varepsilon), \tag{B2}$$

we can use the fact that $[\mathcal{H}(S)]_{S^*} = 0$ to derive the correct curvature jump condition. As was discussed in Sec. II A, we

know that the derivatives Φ, p_Φ, and p_q are bounded. We conclude that these quantities are continuous and that their respective jumps across the point at which the membrane detaches from the particle are zero. Continuity of p_q implies that

$$\lim_{\varepsilon \to 0^+} \lambda(S^* - \varepsilon) \equiv \lambda_- = -2(q'_+ - q'_-). \tag{B3}$$

Upon using λ_- in Eq. (B1) and the fact that $\mathcal{H}$ is constant across S^*,

$$\mathcal{H}_+ - \mathcal{H}_- = (q'^2_+ - q'^2_-) - W + 2(q'_- - q'_+)q'_- = 0, \tag{B4}$$

leading to the only physical extremal solution of the problem:

$$q'_+ - q'_- = -\sqrt{W}. \tag{B5}$$

Note that this condition does not depend on the concentration order parameter Φ. A similar analysis for the case of a spherical particle is straightforward and also yields the condition given by Eq. (B1). This condition was also found in [14] by careful consideration of geometry.

[1] M. Gladnikoff and I. Rousso, Biophys. J. **94**, 320 (2007).
[2] E. Evans and B. Kukan, Blood **64**, 1028 (1984).
[3] D. Needham and R. M. Hochmuth, Biophys. J. **61**, 1664 (1992).
[4] F. M. Hochmuth, J. Y. Shao, J. Dai, and M. P. Sheetz, Biophys. J. **70**, 358 (1996).
[5] R. M. Henderson and H. Oberleithner, Am. J. Physiol. **278**, F689 (2000).
[6] E. Evans and W. Rawicz, Phys. Rev. Lett. **64**, 2094 (1990).
[7] C. Dietrich, M. Angelova, and B. Pouligny, J. Phys. II **7**, 1651 (1997).
[8] H. Lodish, A. Berk, P. Matsudaira, C. A. Kaiser, M. Krieger, M. P. Scott, S. L. Zipursky, and J. Darnell, *Molecular Cell Biology* (Freeman, San Francisco, 2003).
[9] J. Zimmerberg and M. M. Kozlov, Nat. Rev. Mol. Cell Biol. **7**, 9 (2006).
[10] L. V. Chernomordik and M. M. Kozlov, Annu. Rev. Biochem. **72**, 175 (2003).
[11] Z. Chen and R. P. Rand, Biophys. J. **73**, 267 (1997).
[12] S. H. Wu and H. M. McConnell, Biochemistry **14**, 847 (1975).
[13] J. M. Holopainen, M. I. Angelova, and P. K. J. Kinnunen, Biophys. J. **78**, 830 (2000).
[14] R. Rosso and E. G. Virga, Continuum Mech. Thermodyn. **10**, 359 (1998).
[15] U. Seifert and R. Lipowsky, Phys. Rev. A **42**, 4768 (1990).
[16] A. Boulbitch, Europhys. Lett. **59**, 910 (2002).
[17] M. Deserno and T. Bickel, Europhys. Lett. **62**, 767 (2003).
[18] M. Deserno, Phys. Rev. E **69**, 031903 (2004).
[19] S. Das and Q. Du, Phys. Rev. E **77**, 011907 (2008).
[20] V. S. Markin, Biophys. J. **36**, 1 (1981).
[21] U. Seifert, K. Berndl, and R. Lipowsky, Phys. Rev. A **44**, 1182 (1991).
[22] B. Bozic, V. Kralj-Iglic, and S. Svetina,Phys. Rev. E **73**, 041915 (2006).
[23] R. E. Goldstein and S. Leibler, Phys. Rev. A **40**, 1025 (1989).
[24] R. R. Netz and P. Pincus, Phys. Rev. E **52**, 4114 (1995).
[25] W. T. Góźdź and G. Gompper, Phys. Rev. Lett. **80**, 4213 (1998).
[26] T. R. Weikl and R. Lipowsky, Phys. Rev. E **64**, 011903 (2001).
[27] J. M. Allain, C. Storm, A. Roux, M. Ben Amar, and J. F. Joanny, Phys. Rev. Lett. **93**, 158104 (2004).
[28] W. Wiese and W. Helfrich, J. Phys.: Condens. Matter **2**, SA329 (1990).
[29] U. Seifert, Phys. Rev. Lett. **70**, 1335 (1993).
[30] L. Miao, U. Seifert, M. Wortis, and H.-G. Döbereiner, Phys. Rev. E **49**, 5389 (1994).
[31] F. Jülicher and R. Lipowsky, Phys. Rev. E **53**, 2670 (1996).
[32] P. B. Sunil Kumar, G. Gompper, and R. Lipowsky, Phys. Rev. Lett. **86**, 3911 (2001).
[33] T. R. Weikl, M. M. Kozlov, and W. Helfrich, Phys. Rev. E **57**, 6988 (1998).
[34] G. Brannigan and F. L. H. Brown, Biophys. J. **92**, 864 (2007).
[35] P. G. Dommersnes and J. B. Fournier, Eur. Phys. J. B **12**, 9 (1999).
[36] K. S. Kim, J. C. Neu, and G. Oster, Biophys. J. **75**, 2274 (1998).
[37] M. Grabe, J. C. Neu, G. Oster, and P. Nolbert, Biophys. J. **84**, 854 (2003).
[38] R. Lipowsky and H.-G. Döbereiner, Europhys. Lett. **43**, 219 (1998).
[39] P. Sens and M. S. Turner, Biophys. J. **86**, 2049 (2004).
[40] B. J. Reynwar, G. Ilya, V. A. Harmandaris, M. M. Muller, K. Kremer, and M. Deserno, Nature (London) **447**, 461 (2007).
[41] H. Gao, W. Shi, and L. B. Freund, Proc. Natl. Acad. Sci. U.S.A. **102**, 9469 (2005).
[42] I. R. Cooke and M. Deserno, Biophys. J. **91**, 487 (2006).
[43] W. Helfrich, Z. Naturforsch. C **28**, 693 (1973).
[44] P. Sens and S. Safran, Europhys. Lett. **43**, 95 (1998).
[45] T. R. Powers, G. Huber, and R. E. Goldstein, Phys. Rev. E **65**, 041901 (2002).
[46] H.-J. Weber and G. B. Arfken, *Mathematical Methods for Physicists* (Harcourt/Academic, San Diego, 2001).
[47] M. Deserno, M. M. Muller, and J. Guven, Phys. Rev. E **76**, 011605 (2007).
[48] M. M. Müller, M. Deserno, and J. Guven, Phys. Rev. E **76**, 011921 (2007).
[49] J. Kierzenka and L. F. Shampine, ACM Trans. Math. Softw. **27**, 299 (2001).
[50] S. L. Das and J. T. Jenkins, J. Fluid Mech. **597**, 429 (2008).
[51] X. Wang and Q. Du, J. Math. Biol. **56**, 347 (2008).
[52] S. X. Sun and D. Wirtz, Biophys. J. **90**, L10 (2006).
[53] T. Chou, Biophys. J. **93**, 1116 (2007).
[54] J. M. Casasnovas and T. A. Spinger, J. Biol. Chem. **270**, 13216 (1995).
[55] E. Morita and W. I. Sundquist, Annu. Rev. Cell Dev. Biol. **20**, 395 (2004).
[56] I. Pastan and M. C. Willingham, *Endocytosis* (Plenum Press, New York, 1985).